Sustainable Energy & Fuels

ROYAL SOCIETY OF CHEMISTRY

PAPER

Cite this: *Sustainable Energy Fuels*, 2021, **5**, 4041

Simultaneous assistance of molecular oxygen and mesoporous SO_3H–alumina for a selective conversion of biomass-derived furfural to γ-valerolactone without an external addition of H_2†

Surachai Karnjanakom, *[a] Asep Bayu,[b] Panya Maneechakr,[a] Chanatip Samart,[c] Suwadee Kongparakul[c] and Guoqing Guan[d]

The selective conversion of biomass-derived furfural (FF) into γ-valerolactone (GVL) without H_2 consumption is highly interesting due to its explicit utilization as a bio-fuel additive. In this research, we focused on the synthesis of the GVL product *via* simultaneous integration of molecular oxygen and mesoporous SO_3H–alumina catalyst in the presence of 2-butanol as a hydrogen donor. The catalyst was characterized on its chemical–physical properties in order to support catalytic test results. The critical roles of Brønsted–Lewis acid sites in the S–A catalyst, salt addition, ultrasonic irradiation, O_2 and N_2 existences and alcohol solvent as well as kinetic reactions were systematically investigated. As desired using S–A at an *L*/*B* ratio = 0.23, a high yield of GVL (85.6%) was achieved without sustainable formation of humins by the integration of MPV transfer hydrogenation–alcoholysis with *in situ* oxidative degradation. Moreover, the catalyst could be reused for up to twenty runs under oxygen conditions without significant change in its catalytic performance. This work provided a novel strategy for the sustainable production of GVL and the preservation of catalyst reusability.

Received 29th May 2021
Accepted 24th June 2021

DOI: 10.1039/d1se00817j

rsc.li/sustainable-energy

1. Introduction

Currently, the specific synthesis of high-value chemicals and biofuels from renewable resources have attracted a lot of attention in biorefinery industry.[1,2] From this point of view, biomass-derived carbohydrates and/or furfural (FF) can be further utilized as the feedstocks for sustainable production of biofuels and value chemicals such as 5-hydroxymethylfurfural (5-HMF), alkyl levulinate (AL), γ-valerolactone (GVL), 2-(diethoxymethyl)furan (DTMF) and others.[3–6] Among them, the properties of GVL are found to be advantageous in several areas, for instance, (I) it can be applied as a promising renewable chemical in the food and chemical additive industries, (II) it can be considered as a green and nontoxic solvent due to low toxicity and useful polarity properties.[7–9] Commercially, GVL is produced from levulinic acid (LA), furfural (FF), furfuryl alcohol (FA), 5-hydroxymethylfurfural (HMF) or carbohydrates *via* principal reactions such as ethanolysis and etherification over a homogeneous acid catalyst and alcohol as well as H_2 source.[10] Previously, homogeneous catalysts such as HCl, HNO_3 and H_2SO_4 presented excellent catalytic results with advantages such as being inexpensive, fast reaction rate and high product selectivity. However, there are some drawbacks including high toxicity in the environment and complex recycling.[11,12] Also, the external addition of H_2 at high pressure during the reaction process might possibly enhance the production cost in an industrial process. Therefore, the utilization of a heterogeneous catalytic system is highly desirable in the current state.

To date, several heterogeneous acid catalysts consisting of Lewis and Brønsted acid sites have been developed for GVL production.[13–16] Gao *et al.*[17] studied the GVL production from FF over the Fe_3O_4/ZrO_2@MCM-41 catalyst, and the results found that the GVL yield of ~81% was obtained at 150 °C for 24 h. Li *et al.*[18] achieved without an external source of H_2, the conversion of FF into GVL (GVL yield = 80%) at 150 °C for 18 h over a Zr-P/SAPO-34 catalyst. Peng *et al.*[19] found that a maximum GVL yield of 72.4% was obtained from FF conversion catalyzed by FM-Zr-ARS at 160 °C for 8 h *via* intermediate CTH reaction steps. They also reported that a combination of Lewis and Brønsted acid sites on the as-prepared catalyst resulted in the facile production of GVL *via* the last step of ring-opening in alkyl furfuryl ether (AFE) with transfer hydrogenation/lactonization.

[a]*Department of Chemistry, Faculty of Science, Rangsit University, Pathumthani 12000, Thailand. E-mail: surachai.ka@rsu.ac.th; surachaikarn@gmail.com*

[b]*Research Center for Biotechnology, Indonesian Institute of Sciences (LIPI), Jalan Raya Jakarta-Bogor KM. 46, Cibinong, Bogor, West Java, Indonesia*

[c]*Department of Chemistry, Faculty of Science and Technology, Thammasat University, Pathumthani 12120, Thailand*

[d]*Energy Conversion Engineering Laboratory, Institute of Regional Innovation (IRI), Hirosaki University, 2-1-3, Matsubara, Aomori 030-0813, Japan*

† Electronic supplementary information (ESI) available. See DOI: 10.1039/d1se00817j

Unluckily, to obtain a high GVL yield from FF conversion, a long reaction time, high reaction temperature and high pressure as well complex/expensive system are needed. Furthermore, the co-formation of humins (unwanted product) in liquid solution and on the catalyst surface *via* polymerization always occurred, leading to simultaneous reduction of catalyst stability and GVL yield.[20–22]

As mentioned above, a green catalytic system with contributions from ultrasonic irradiation/oxygen molecular/stable mesoporous catalyst was applied to solve those problems. Up to date, several kinds of mesoporous materials present excellent properties for catalytic applications.[23–25] Since they have a high surface area, porosity and large pore size, substances or intermediates can easily diffuse and access active sites of catalyst without blockage. Thus, it can be considered to apply as support and/or catalyst for our research. Herein, we developed the ordered mesoporous SO_3H–alumina (S–A) catalyst consisting of Lewis and Brønsted acid sites with an optimal ratio *via* hydrothermal and functionalization processes in the presence of Pluronic P123 surfactant and chlorosulfonic acid (CA). The physical–chemical properties of the catalyst were analyzed by N_2 sorption/BET-BJH, XRD, SEM-EDS, FT-IR, XPS, TGA-DTG and TPD techniques. The additional loadings of alcohol solvent and inorganic salt, as well as the use of O_2 and N_2 during the reaction process, were tested in order to know that how can suppress the co-formation of humins during GVL production. The ultrasonic application was studied and compared with a conventional system to support the reaction rate for GVL production. Catalytic reaction pathways in each step for GVL production were purposed together with the kinetic reaction model. The catalytic activity based on the turnover rate of S–A was compared with commercial SO_3H-functionalized materials. Catalyst recycling was tested and regenerated under O_2 and N_2 conditions. To the best of our knowledge, this study not only reports the sustainable production of GVL with high yields with the preservation of catalyst stability but also presents catalytic reaction pathways in each step under the developed process.

2. Experimental

2.1. Preparation of mesoporous SO_3H–alumina catalyst

Mesoporous alumina was prepared following Pluronic P123-assisted hydrothermal conditions and followed by the calcination process.[26] The molar compositions applied for S–A synthesis are as follows: 1.0Al : 0.25P123 : 85H_2O : 4.6urea. In a typical synthesis, certain amounts of $Al(NO_3)_3 \cdot 9H_2O$ and urea were dissolved in 45 mL of DI water and stirred at 35 °C for 30 min to form a clear solution. Then, Pluronic P123 was mixed in the as-prepared solution and continuously stirred at 35 °C for ~1 h to obtain a homogeneous solution. The resultant mixture was further transferred to a Teflon-lined autoclave size 100 mL, which was sealed and placed in an oven at 150 °C for 12 h. Thereafter, the precipitate or boehmite was filtered, washed with DI water until pH = 7, and dried in an oven at 110 °C, overnight. Lastly, it was calcined at 650 °C for 2 h to remove the template and to rearrange the ordered-mesoporous structure.

For the functionalization process, 1.0 g of mesoporous alumina was introduced in 20 mL of dichloromethane under set-up consisting of suction equipped with a dropping funnel and stirred for 5 min. Here, the gas outlet was set with a vacuum system + $CaCl_2$ trap. Then, a certain amount of chlorosulfonic acid was wisely dropped into a mixture solution and stirred for 2 h under ambient temperature. The surplus HCl produced during the functionalization reaction was easily removed by the suction system. After finishing the process, the obtained mesoporous rod-like SO_3H–alumina (S–A) was filtered, washed with alcohol with DI water, and dried in an oven at 110 °C overnight. Here, the different weight ratios of chlorosulfonic acid to alumina (0 : 1, 1 : 1, 2 : 1, 3 : 1 and 4 : 1) were studied to find the best condition for catalytic production of GVL. The details of the catalyst characterization techniques are given in the ESI.†

2.2. Catalytic production of GVL

The catalytic test for GVL production was performed in a three-neck round bottom flask equipped with an ultrasonic probe, a reflux condenser, and a gas tube. In a typical run, 20.8 mmol of FF and 0.1 g of LiCl and 20 mL of 2-butanol were mixed with 1.5 g of catalyst, and transferred to a flask. Then, the reaction was carried at 120 °C for 4 h at a stirring speed of 650 rpm with an ultrasonic frequency at 2500 Hz. During the reaction process, O_2 or N_2 gas was flushed inside the reactor at a flow rate of 20 mL min^{-1}. It should be mentioned here that ultrasonic generation condition was performed using an ultrasonic probe sonicator (Athena Technology) while stirring and heating processes were controlled using a hot plate magnetic stirrer (C-MAG-HS7, IKA, GERMAN).

Here, various effects including weight ratios of chlorosulfonic acid to alumina, type of inorganic salt, LiCl amount, ultrasonic power, ultrasonic duty cycle, and O_2 or N_2 atmosphere for GVLL production were systematically studied. It should be mentioned here that some general factors such as catalyst amount, 2-butanol amount, reaction temperature and time were fixed for all experiments based on our preliminary studies *via* the optimization process using a statistical RSM analysis.[27] After the complete process, the reaction was terminated by soaking in the ice bath, and then the spent catalyst was separated from the liquid products by filtration and centrifugation processes as well as washing by ethanol and DI water several times. Lastly, the catalyst was dried in an oven at 110 °C, overnight before reusability and characterization tests.

2.3. Liquid product analysis

Substrate and liquid products were qualitatively analyzed using gas chromatography (Agilent instrument) equipped with a flame ionization detector (GC-FID) including a capillary Agilent HP-5 column (30.0 m × 0.25 mm × 0.25 μm). The temperature program was as follows: 313 K (4 min) – 5 K min^{-1} – 523 K (5 min).[21] N_2 was utilized as carrier gas at a flow rate of 1.0 mL min^{-1}. The concentrations of each product were calculated using dodecane as an internal standard. The FF conversion and product yield and selectivity were calculated using the following eqn (1)–(3):

$$\text{FF conversion}\,(\%) = \frac{\text{mole percentage of FF reacted}}{\text{mole percentage of initial FF}} \times 100 \quad (1)$$

$$\text{Product yield}\,(\%) = \frac{\text{mole percentage of product produced}}{\text{mole percentage of initial FF}} \times 100 \quad (2)$$

$$\text{Product selectivity}\,(\%) = \frac{\text{mole percentage of product produced}}{\text{mole percentage of FF reacted}} \times 100 \quad (3)$$

3. Results and discussion

3.1. Critical roles for conversion of FF into GVL

Details on the textural, structure, morphological and chemical properties of S–A catalysts are provided in ESI (Fig. S1–S6†).[28–36] Fig. 1 shows the role of the weight ratio of chlorosulfonic acid to alumina on catalytic conversion of FF into GVL and other chemicals under the O_2 atmosphere. Herein, the chemical selectivities produced from FF conversion are classified into six types such as GVL, 2-butyl levulinate (BL) 2-butyl furfuryl ether (BFE), FA, DTMF and humins. In the absence of an S–A catalyst, GVL products were not produced although the FF conversion reached 47.3%. Unlikely, DTMF was easily produced to form surrogates by ultrasonic-assisted acetalization between FF and 2-butanol. However, after using the S–A (0 : 1) catalyst, FF could be transformed into GVL with a slight yield of 20.2% but the DTMF selectivity was significantly decreased on increasing of BFE and BL selectivities. This suggests that only Lewis acid sites in mesoporous alumina could suppress the acetalization reaction of FF, and further shifted into Meerwein–Ponndorf–Verley (MPV) transfer hydrogenation and alcoholysis reactions based on the tandem reaction pathways using 2-butanol as a hydrogen donor. The presence of Lewis–Brønsted acid sites with different ratios and acidic properties of S–A catalysts was determined from NH_3–TPD analysis, and the results are shown in Table 1. For pristine S–A (0.1), only Lewis acid site/weak acid sites with acidity of 0.45 mmol g^{-1} were detected. Interestingly, with the increase in weight ratios of chlorosulfonic acid to alumina from 1.1 to 4 : 1, their acidities were also increased to some extent with the significant reduction of *L*/*B* ratios from 0.58 to 0.10. This should be resulting from the regeneration of Brønsted acid sites/strong acid sites, obtained from the functionalization process.[37–40] However, the number of Lewis acid sites for S–A (4 : 1) was seriously lower, while the other one was well kept constant. This phenomenon should be described based on the existence of sulfonic groups with too much amount tremendously coated on the S–A catalyst surface. Here, the different distributions of acid sites could be attributed to the acidity amount, the presence of different acid sites as well as sulfonic acid groups located at different places in mesoporous rod-like alumina structure. As such from the obtained catalytic results, the increase in weight ratios of chlorosulfonic acid to alumina from 1.1 to 3 : 1 resulted in the facile formation of GVL with its increasing from 42.1 to 85.6%, resulting from the increase of acidity, especially for Brønsted acid site, which was highly favored for etherification, hydrolytic ring-opening and lactonization reactions.[41] Unfortunately, GVL was then decreased to some extent using S–A (4 : 1). This phenomenon should be attributed to the further conversion of GVL into humins *via* polymerization/condensation reactions catalyzed by supernumerary acidity of the S–A catalyst. This indicates that the synergistic effect of sulfonic group/Brønsted acid with Lewis acid sites on mesoporous alumina was very important for catalytic production of GVL. From these results, S–A (3 : 1) catalyst was selected as a catalyst with the optimal ratio for further studies.

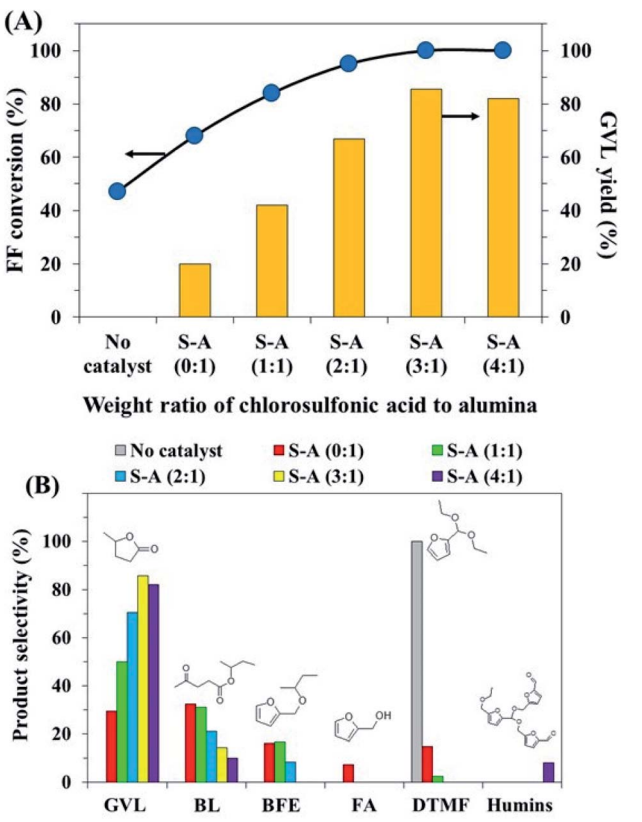

Fig. 1 Role of weight ratio of chlorosulfonic acid to alumina on conversion of FF into GVL under O_2 atmosphere. Reaction conditions: catalyst amount = 1.5 g, reaction temperature = 120 °C, reaction time = 4 h, ultrasonic energy = 90 W and ultrasonic duty cycle = 60%.

Fig. 2A and B show the role of inorganic salts on the conversion of FF into GVL over the S–A catalyst under the O_2 atmosphere. Here, various loadings of monovalent and divalent ions were evaluated in the catalytic system. For no salt loading, only ~43% of GVL yield was obtained, indicating that the salt loading was very necessary for the catalytic system. As expected, the GVL yield/selectively could be efficiently increased with inorganic salt loading, probably due to salting out influence and supporting the reaction selectivity in the solution system. The selectivity for catalytic production of GVL was in the order of $Li^+ > Na^+ > K^+$ when chloride anions were fixed, indicating that the selectivity for GVL

Table 1 Physicochemical properties of various catalysts

Catalyst	Surface area ($m^2\ g^{-1}$)	Pore volume ($cm^3\ g^{-1}$)	Pore size (nm)	Acidity (mmol g^{-1})	Lewis acid amount (mmol g^{-1})	Brønsted acid amount (mmol g^{-1})	*L*/*B* ratio
S–A (0 : 1)	561	0.82	3.14	0.45	0.45	0.00	—
S–A (1 : 1)	544	0.75	3.12	1.17	0.43	0.74	0.58
S–A (2 : 1)	529	0.69	3.12	1.86	0.42	1.44	0.29
S–A (3 : 1)	515	0.62	3.11	2.28	0.43	1.85	0.23
S–A (4 : 1)	486	0.54	3.08	2.95	0.28	2.67	0.10
Spent S–A (3 : 1)[a]	502	0.61	3.09	2.24	0.41	1.83	0.22
Spent S–A (3 : 1)[b]	216	0.04	1.45	2.21	0.37	1.84	0.20

[a] Spent catalyst after recycling test for 20 cycles under O_2 atmosphere. [b] Spent catalyst after recycling test for 20 cycles under N_2 atmosphere.

production was dependent on the cationic radius. In the case of various anion natures with a fixed Li^+ counterion, the formation rate of GVL was in the order of $Cl^- > Br^- > NO_3^- > SO_4^{2-}$. Here, the ability of these ions for the conversion of FF into GVL was attributed to the proffering of electron density to the carbon atoms of FF, suppressing polymerization/condensation reactions for humins formation.[42] The lowest selectivity for GVL formation was found using a sulfate ion, resulting from participation in hydrogen bonds/water molecules and carbonyl–hydroxyl groups of FF or FA, leading to the facile formation of side reaction intermediates.[43] Fig. 2C and D show the role of LiCl adding amount on the conversion of FF into GVL over S–A catalyst under O_2 atmosphere. The GVL yield/selectivity was increased based on the increase of LiCl amount. Here, a maximum GVL yield/selectivity was obtained at a saturated point with 0.1 g of LiCl amount. This phenomenon could be described as improving the interaction between the immiscibility of the solvent phase with molecular bonds in the chemical intermediates, thus supporting in dispersion rate in the organic phase.[44]

Fig. 3A and B show the role of ultrasonic power on the conversion of FF into GVL over S–A catalyst under O_2 atmosphere. With the generation of ultrasonic power from 50 to 90 W, a dramatic increase in GVL yield from 38.9 to 85.6% was obtained, suggesting that a higher generation of ultrasonic power supplemented the selective conversion of FF into GVL owing to facile protonation on carbonyl–hydroxyl groups of FF/FA *via* interaction at active sites of the S–A catalyst. Also, the level of cavitation bubbles formed in the reaction medium system was related to increasing ultrasonic power, improving the environmental conversion of FF. In the case without

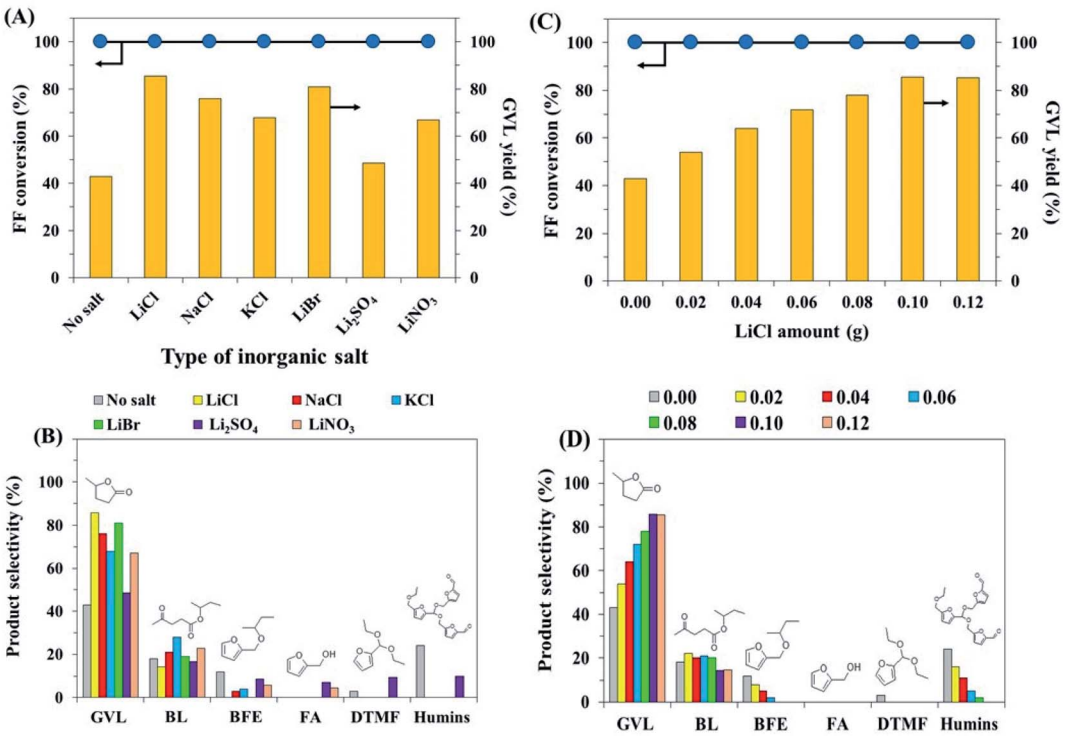

Fig. 2 Roles of (A and B) inorganic salt type and (C and D) LiCl amount on conversion of FF into GVL under O_2 atmosphere. Reaction conditions: catalyst amount = 1.5 g, reaction temperature = 120 °C, reaction time = 4 h, ultrasonic energy = 90 W and ultrasonic duty cycle = 60%.

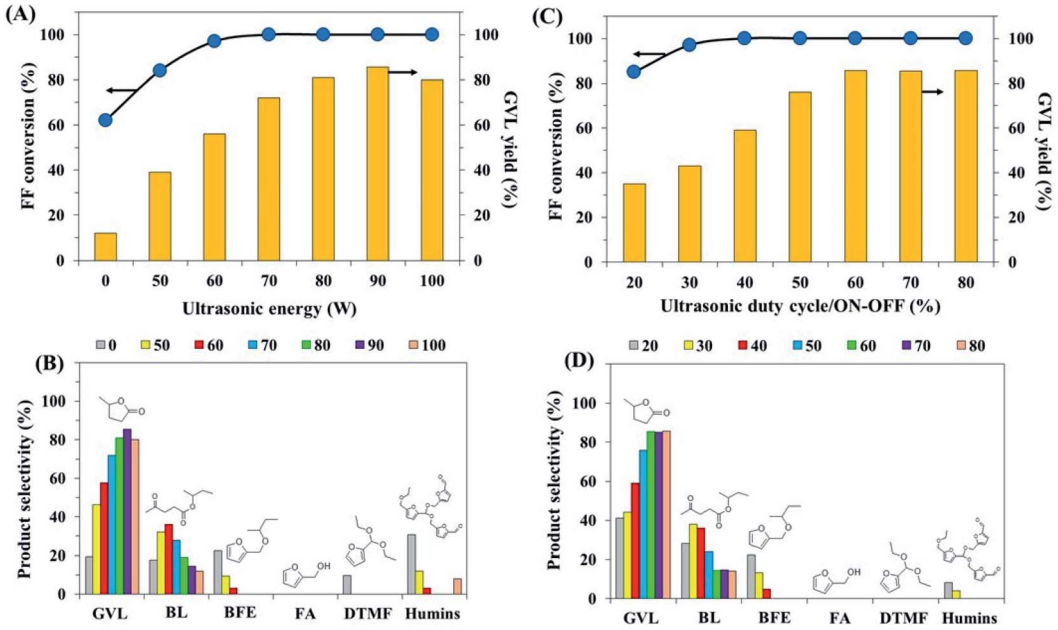

Fig. 3 Roles of (A and B) ultrasonic energy and (C and D) ultrasonic duty cycle on the conversion of FF into GVL under O_2 atmosphere over S–A catalyst. Reaction conditions: catalyst amount = 1.5 g, reaction temperature = 120 °C and reaction time = 4 h.

ultrasonic power, only a GVL yield of ~12% was formed, while several selectivities of unwanted products such as humins, BL and DTMF were easily formed. Interestingly, checking the color characteristics, the conventional reaction method showed a deep-dark color for the spent catalyst and liquid products, which was totally opposite to what was observed in the ultrasonic reaction system. This indicates that ultrasound assistance not only improved the reaction rate but it also suppressed the formation of humins, and maintain the catalyst stability. However, further increase of ultrasonic power from 90 to 100 W resulted in the facile condensation of GVL into humins, leading to the slight reduction of GVL yield from 85.6 to 80.2%. Fig. 3C and D show the role of the ultrasonic duty cycle on the conversion of FF into GVL over S–A catalyst under O_2 atmosphere. In this study, various ON–OFF times of ultrasonic irradiation were defined under the number of ultrasonic duty cycles, for instance, a duty cycle number of 80% was assigned as 8 s on-time and followed by 2 s off-time with ultrasonic generation. This duty was applied to estimate the dispensable electrical energy consumption. As obtained, the GVL yield was increased from 35.0 to 85.6% upon increasing the duty cycle from 20% (2 s ON/8 s OFF) to 60% (6 s ON/4 s OFF), then an insignificant difference in GVL yield was observed for the duty cycle at 70%. Here, the catalytic upgrading process of FF could be promoted *via* mass transfer/interfacial area in cushioning of the cavity collapse at intermediates toward a swift selectivity rate.[45] Thus, an ultrasonic power of 90 W at a duty cycle of 60% was determined as an optimal power generation.

3.2. Reaction route for FF conversion into various products

Fig. 4A shows the catalytic behavior of humins formation on the spent S–A catalyst *versus* reaction time on the conversion of FF into GVL under O_2 and N_2 conditions. Here, the weight loss at the temperature range of 100–400 °C was investigated to describe on humins decomposition from the spent catalyst. The content of humins deposited on the surface of the spent S–A catalyst under N_2 conditions was more than when compared under the O_2 atmosphere. Furthermore, the liquid product under N_2 conditions was also deep-dark while O_2 condition was light yellow. More interestingly, the amount of humins formation on the spent catalyst was continuously reduced until its natural color was gradually restored with increasing of the reaction time from 10 to 60 min under O_2 conditions. In contrast, this result was the opposite trend when compared with the N_2 conditions, indicating that the existence of O_2 could maintain the long-term stability of the S–A catalyst and avoid the humins formation during the reaction process *via* oxidative degradation.[46] To support these data, we tried to perform catalytic testing at 1st cycle under N_2 conditions and then retested in the 2nd cycle after the treatment under O_2 conditions without adding FF. As obtained, the dark-brown catalyst was almost absolutely restored to pristine color and its catalytic performance was effectively recovered. DTG thermograms of spent S–A catalysts after reaction time 30 min are shown in Fig. 4B. DTG profiles of spent S–A catalysts showed different thermal decomposition ranges of humins, suggesting that the deposition state of humins on spent catalysts had some different behavior. The reaction under N_2 conditions resulted in the facile formation of hard humins species on the spent catalyst, which could be observed at a higher thermal decomposition range of the DTG profile, while a lower decomposition temperature range was soft humins species (O_2 condition). Here, the humins deposited on the S–A catalyst under O_2 were more easily eliminated. In contrast, the humins formed under N_2 conditions were difficult to be decomposed. From these

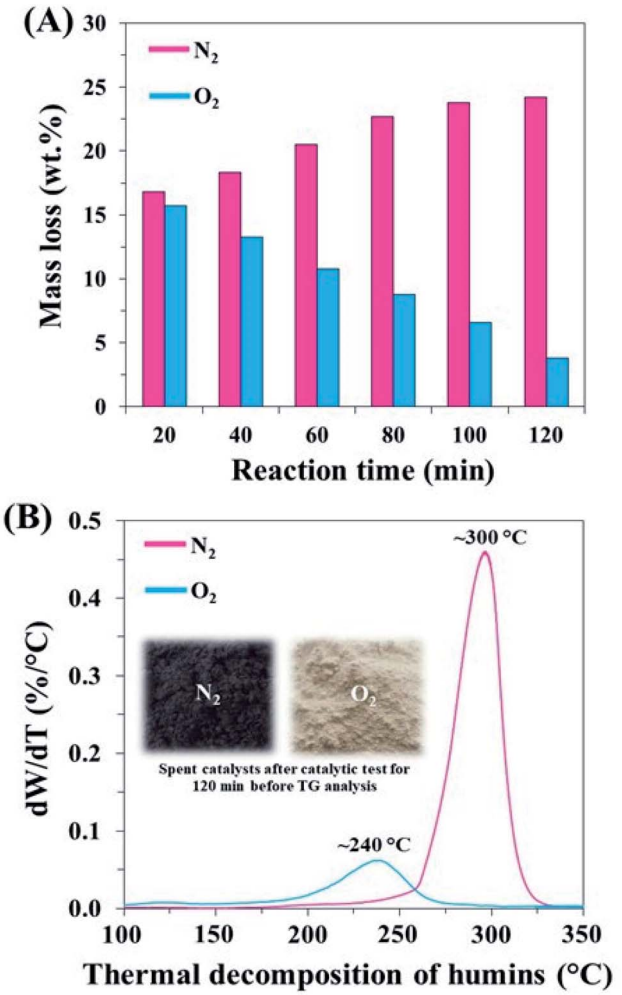

Fig. 4 (A) Role of humins deposited on the spent S–A catalysts *versus* reaction time, (B) DTG profiles of spent S–A catalysts after a reaction time of 120 min on the conversion of FF into GVL under O_2 and N_2 atmospheres.

results, *in situ* removal/suppression of humins could occur in the existence of molecular O_2, which was easier to be regenerated at a lower calcination temperature.

The possible reaction pathways for the conversion of FF into GVL and other chemicals over S–A catalyst *via* the main tandem reaction system, including transfer hydrogenation, etherification–ethanolysis and hydrolytic ring-opening are summarized and illustrated in Fig. 5. Here, 2-butanol could serve as a hydrogen donor for assisting MPV transfer hydrogenation.[47] In other words, high efficiency for *in situ* production of H* species was from alcohols. The first step, the existence of the Lewis acid site in the S–A catalyst could promote the transfer hydrogenation of FF to FA.[48] In the case without the catalyst addition, the reversible acetalization for facile conversion of FF into DTMF easily occurred with ultrasonic assistance. Afterward, BFE was further formed from FA etherification with 2-butanol in the presence of Lewis or Brønsted acid sites of the S–A catalyst. Meanwhile, BL product was produced from hydrolytic ring-opening of BFE catalyzed by Brønsted acid site with a suitable amount. Finally, BL was converted into GVL *via* second transfer hydrogenation followed by lactonization. As is known, ultrasound generation could crack the O–H bond in the water molecule derived *in situ* production to form hydrogen radicals with hydroxyls ($H_2O/^{\bullet}H + {}^{\bullet}OH$).[49] The existence of abundant radicals and oxidizing species could attack the chains in the FF structure, resulting in the improvement of the reaction system. According to Le Chatelier's principle, an excessive amount of alcohol was required in order to shift the equilibrium forward to the GVL product. From an economic perspective, the remaining amount of alcohol after finishing the reaction process could be recovered by the evaporation technique. When the too low ratio of *L*/*B* was applied, such as S–A (4 : 1) with an *L*/*B* ratio of 0.1, unwanted products could be easily produced, leading to a reduction of GVL yield. In this case, polymerization/condensation could be activated to produce humins. Moreover, the formation ability of hard humins species could be effectively suppressed *via* oxidative degradation by the introduction of oxygen.

Based on such reaction pathways, kinetic behavior was further studied for conversion of FF to BFE, BL and GVL over the S–A catalyst in the existence of 2-butanol at different temperatures (333–393 K). It should be noted that since 2-butanol was used in much more amount than other components, the reaction rate constants in each step (k_1, k_2 and k_3) were thus fixed from the pseudo-first order model as shown in the following eqn (4)–(7):[17,19]

$$\frac{dC_{FF}}{dt} = -k_1 C_{FF} \quad (4)$$

$$\frac{dC_{BFE}}{dt} = k_1 C_{FF} - k_2 C_{BFE} \quad (5)$$

$$\frac{dC_{BL}}{dt} = k_2 C_{BFE} - k_3 C_{BL} \quad (6)$$

$$\frac{dC_{GVL}}{dt} = k_3 C_{BL} \quad (7)$$

To calculate the activation energy (E_a) during catalytic conversions of FF to BFE, BL and GVL, the Arrhenius model was applied as shown in eqn (8):

$$k_i = A \exp\frac{-E_a}{RT} \quad (8)$$

The overall kinetic reaction processes under ultrasonic and conventional autoclave systems were simplified as shown in Fig. 6. The proposed models had an excellent fit for the experimental data for both systems. Here, the rate constant (k_1) for MPV transfer hydrogenation–etherification of FF to BFE presented the fastest of all the catalytic steps while the cascade conversion of BL to GVL was significantly lower than that of the other one under identical temperatures (Fig. 6A and B). This suggests that lactonization of BL to GVL represented a rate-limiting step during this reaction. In addition, as expected, the ultrasonic system well provided a higher reaction rate constant for all steps than conventional autoclave systems. The

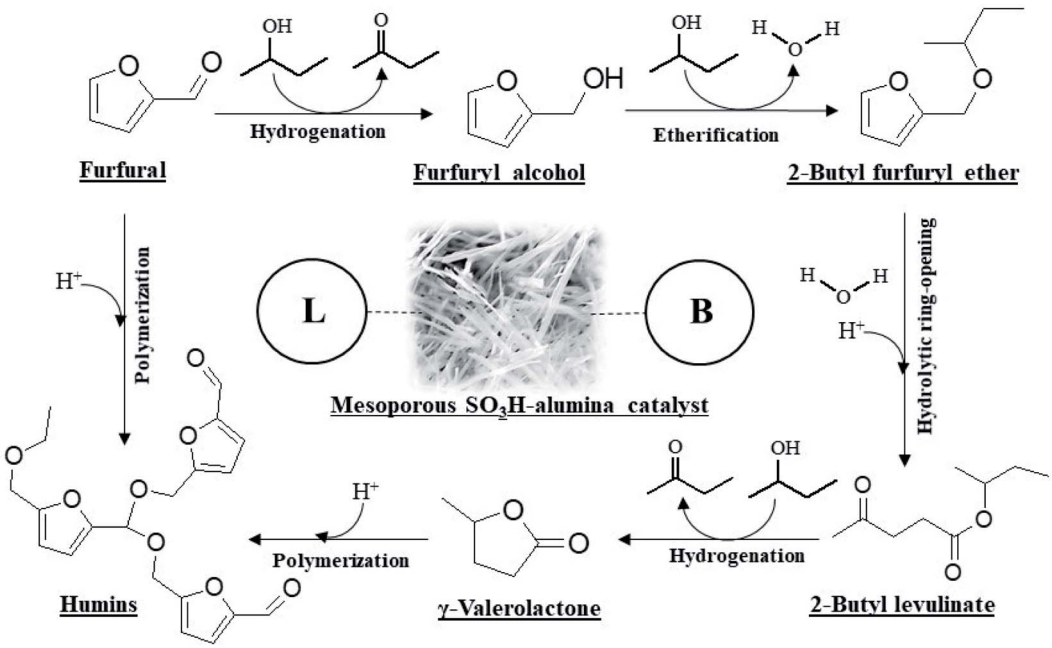

Fig. 5 Reaction pathways for catalytic conversion of FF into GVL and other products in the presence of 2-butanol.

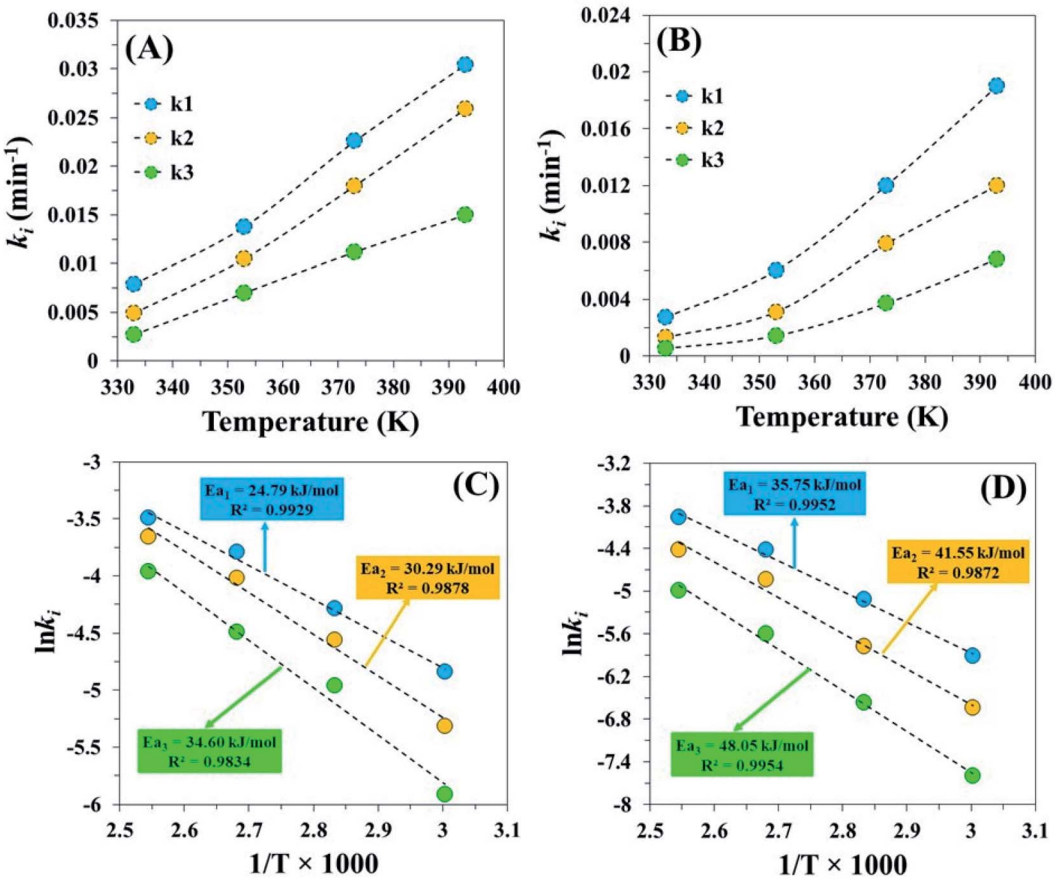

Fig. 6 Kinetic plots of reaction rate constants in each step *versus* temperatures under (A) ultrasonic condition and (B) conventional condition. Arrhenius plots of reaction rate constants using a function of reaction temperature under (C) ultrasonic condition and (D) conventional condition.

apparent activation energies derived from the ultrasonic system of E_{a_1}, E_{a_2}, and E_{a_3} were 24.79, 30.29 and 34.60 kJ mol^{-1}, which were lower than those for the conventional autoclave systems (Fig. 6C and D). Similarity for both systems, FF was easily transformed to BL due to the lowest activation energy, while BL-to-GVL was hardest due to the highest activation energy. Here, the evident activation energies determined in this study were followed by a kinetically controlled regimen, as appraised by the Weisz–Pratercriterion factor, indicating the no mass-transfer limitations interfered. To update our obtained results, a comparison of each catalytic system for GVL production from the FF substrate is shown in Table 2.[17–20] It should be mentioned here that FF is still interesting as a starting substrate since a few previous studies are found, comparing it with AL or LA. As expected, our S–A catalyst presented greater catalytic performance than Fe_3O_4/ZrO_2@MCM-41, Zr-P/SAPO-34, FM-Zr-ARS and Zr-CN/H-β. This might be attributed to its remarkable properties, such as high surface area, large pore size, high stability, an optimal ratio of *L*/*B* and high acidity (Table 2, entries 1–4 *vs.* 7). More interestingly, a much shorter reaction time and lower reaction temperature for GVL production were clearly found using an ultrasonic system, compared with autoclave and conventional reflux systems (entries 1–4, 6–9 *vs.* 5). This confirms that our catalytic system had good effectiveness for the sustainable production of GVL.

Since alcohols could serve as solvent and H-donor in the MPV transfer hydrogenation, the conversion of FF into GVL over the S–A catalyst using various types of alcohols was also investigated, and their results are shown in Table 3. One can see that the formation ability of L products was more difficult when carbon number in alcohols was increased. The formation rate of GVL was in the order of 2-butanol > 2-pentanol > 2-propanal > 1-butanol > 1-pentanol > 1-propanol > ethanol > methanol, while the formation rate of AL had the opposite trend. Here, AL formation was most favored for primary alcohols, especially for methanol. Moreover, GVL was less preferred to produce primary alcohols than secondary alcohols, suggesting that the second transfer hydrogenation was promoted *via* lower reduction potential in secondary alcohol for GVL production. This difference should be described on the interaction level between carbonyl compounds with alcohols based on the data of standard molar enthalpy in the report of Waal *et al.*[50] It is known that low reduction potential could lead to a more available detachment of hydrogen in alcohol, so that is why the transfer hydrogenation reaction was much easier to promote. However, even 2-pentanol had the lowest reduction potential, but lower GVL yield was found on it when compared with 2-butanol. It is possible that the steric hindrance value of 2-pentanol was higher than that of 2-butanol, resulting in retardation of intermediate esters.[18] This study provided an alternative way for selective conversion of FF into GVL or AL using different alcohols.

Table 3 Effect of various alcohols for production of AL and GVL under O_2 atmosphere over S–A catalyst[a]

Entry	Alcohol type	Conversion (%)	AL yield (%)	GVL yield (%)
1	Methanol	100	52.1	47.9
2	Ethanol	100	45.3	54.7
3	1-Propanol	100	38.8	61.2
4	2-Propanol	100	22.5	77.5
5	1-Butanol	100	34.2	65.8
6	2-Butanol	100	14.4	85.6
7	1-Pentanol	100	30.5	63.9
8	2-Pentanol	100	11.7	82.1

[a] Reaction conditions: catalyst amount = 1.5 g, reaction temperature = 120 °C, reaction time = 4 h, ultrasonic power = 90 W and ultrasonic duty cycle = 60%.

3.3. Catalyst reusability

To confirm the long-term stability under as-obtained optimal conditions, the S–A catalyst was reused for 20 cycles under O_2 and N_2 atmospheres without the regeneration process (Fig. 7A). It is found that the catalytic performance under N_2 was obviously decreased from 1st to 20th cycle, leading to a drastic reduction of GVL yield from 78.4 to 3.3%. In contrast, the catalyst under O_2 kept its long-term stability for 20 cycles with a small decrease of GVL yield (~3%). This exactly confirms that the existence of O_2 could preserve the catalyst stability during the reaction by suppressing the formation/deposition of humins on the spent catalyst. For N_2 conditions, a large number of hard humins species easily formed and deposited on spent catalysts could lead to the rapid deactivation of the catalyst. In the other words, the humins covered on the catalyst caused the blockage of pores, resulting in poor accessibility at active sites.[51] However, the spent catalyst could be regenerated by the

Table 2 Comparison in our catalytic performances with previous references for conversion of FF into GVL

Entry	Catalyst	Temperature (°C)	Time (h)	Catalytic system	GVL yield (%)	Ref.
1	Fe_3O_4/ZrO_2@MCM-41	150	24	Autoclave system + air condition	80.8	17
2	Zr-P/SAPO-34	150	18	Autoclave system + N_2 condition	80.0	18
3	FM-Zr-ARS	160	8	Autoclave system + N_2 condition	72.4	19
4	Zr-CN/H-β	160	18	Autoclave system + air condition	76.5	20
5	S–A (3 : 1)	120	4	Ultrasonic system + O_2 condition	85.6	This work
6	S–A (3 : 1)	120	4	Autoclave system + O_2 condition	53.2	This work
7	S–A (3 : 1)	120	12	Autoclave system + O_2 condition	77.8	This work
8	S–A (3 : 1)	120	4	Reflux system + O_2 condition	24.7	This work
9	S–A (3 : 1)	120	24	Reflux system + O_2 condition	78.2	This work

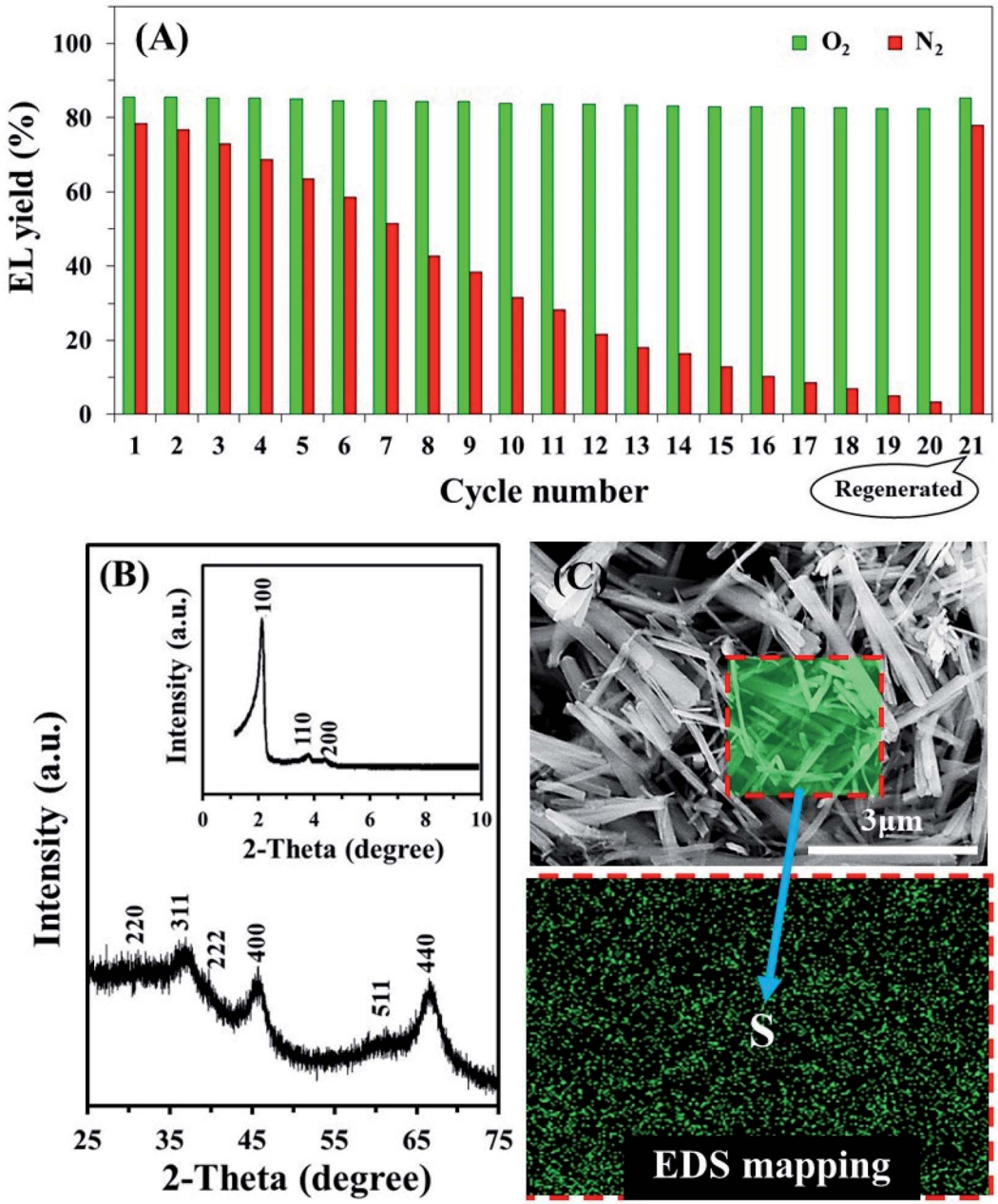

Fig. 7 (A) Reusability, long-term stability and regeneration performance of S–A catalyst for conversion of FF into GVL under O_2 and N_2 atmospheres, (B) XRD pattern and (C) SEM-EDS mapping image of spent S–A catalyst regenerated after recycling test for 20 cycles under O_2 atmosphere.

calcination process at 350 °C, and catalytic performance result (21st cycle) was perfectly recovered as same as the 1st cycle. This indicates that only deposition of humins was the main problem for catalyst deactivation while significant leaching of active sulfonic species on the catalyst did not occur. To support our assumption, the textural properties of spent catalysts are provided in Table 1. No significant leaching of acidic amount on the spent catalyst was clearly detected, but the surface area, pore volume and pore size were strongly decreased from humin deposition under only N_2 conditions. In addition, the ordered-mesoporous structure of the spent catalyst was still preserved during the reusability test for 20 cycles while its fiber-like morphology with distribution trend of sulfonic groups did not change as confirmed from XRD and SEM-EDS results (Fig. 7B and C). Therefore, it could be summarized that our catalytic system is very effective and reusable.

4. Conclusion

The S–A catalyst consisting of Brønsted–Lewis acid sites was applied in the catalytic conversion of FF into GVL. The S–A synthesized by optimal weight ratio of chlorosulfonic acid to

alumina (3 : 1) had excellent properties such as high surface area, large pore size and high acidity (L/B ratio = 0.23). The interesting factors such as acidity/acid site, inorganic salt addition, ultrasonic generation, O_2 condition and alcohol solvent had a significant effect on the selective production of GVL. The addition of O_2 in the catalytic system was highly expedient in suppressing the humins formation in liquid products and on the catalyst. The amount of humins deposited on the spent catalyst easily increased with increasing reaction time under N_2 conditions. The excessive amount of Brønsted acid site in S–A (4 : 1) promoted side reactions such as condensation/polymerization to form humins. Secondary alcohols such as 2-propanol, 2-butanol and 2-pentanol favored in second transfer hydrogenation of EL into GVL. A maximum GVL yield of 85.6% was achieved under low activation energy. The long-term stability of the catalyst for 20 cycles with a few reducing of GVL yield was achieved without significant leaching of the sulfonic group.

Conflicts of interest

There are no conflicts to declare.

Acknowledgements

The authors would like to gratefully appreciate Department of Chemistry, Faculty of Science, Rangsit University, Thailand for supporting all chemicals, equipment and instruments.

References

1 M. Limlamthong and A. C. K. Yip, Recent advances in zeolite-encapsulated metal catalysts: A suitable catalyst design for catalytic biomass conversion, *Bioresour. Technol.*, 2020, **297**, 122488.

2 F. Zaccheria, F. Bossola, N. Scotti, C. Evangelisti, V. D. Santo and N. Ravasio, On demand production of ethers or alcohols from furfural and HMF by selecting the composition of a Zr/Si catalyst, *Catal. Sci. Technol.*, 2020, **10**, 7502–7511.

3 P. Maneechakr and S. Karnjanakom, Catalytic conversion of fructose into 5-HMF under eco-friendly-biphasic process, *React. Chem. Eng.*, 2020, **5**, 2058–2063.

4 S. Dutta, I. K. M. Yu, D. C. W. Tsang, Y. H. Ng, Y. S. Ok, J. Sherwood and J. H. Clark, Green synthesis of gamma-valerolactone (GVL) through hydrogenation of biomass-derived levulinic acid using non-noble metal catalysts: A critical review, *Chem. Eng. J.*, 2019, **372**, 992–1006.

5 Z. H. He, C. S. Jiang, Z. Y. Wang, K. Wang, Y. C. Sun, M. Q. Yao, Z. H. Li and Z. T. Liu, Catalytic hydrodeoxygenation of biomass-derived oxygenates to biofuels over Co- based bimetallic catalysts, *Sustainable Energy Fuels*, 2020, **4**, 4558–4569.

6 P. L. Arias, J. A. Cecilia, I. Gandarias, J. Iglesias, M. L. Granados, R. Mariscal, G. Morales, R. M. Tost and P. M. Torres, Oxidation of lignocellulosic platform molecules to value-added chemicals using heterogeneous catalytic technologies, *Catal. Sci. Technol.*, 2020, **10**, 2721–2757.

7 P. Rani and R. Srivastava, Integration of a metal–organic framework with zeolite: a highly sustainable composite catalyst for the synthesis of γ-valerolactone and coumarins, *Sustainable Energy Fuels*, 2018, **2**, 1287–1298.

8 S. Pendem, I. Mondal, A. Shrotri, B. S. Rao, N. Lingaiah and J. Mondal, Unraveling the structural properties and reactivity trends of Cu–Ni bimetallic nanoalloy catalysts for biomass-derived levulinic acid hydrogenation, *Sustainable Energy Fuels*, 2018, **2**, 1516–1529.

9 P. Sudarsanam, R. Zhong, S. V. D. Bosch, S. M. Coman, V. I. Parvulescu and B. F. Sels, Functionalised heterogeneous catalysts for sustainable biomass valorisation, *Chem. Soc. Rev.*, 2018, **47**, 8349–8402.

10 B. Jia, C. Liu and X. Qi, Selective production of ethyl levulinate from levulinic acid by lipase-immobilized mesoporous silica nanoflowers composite, *Fuel Process. Technol.*, 2020, **210**, 106578.

11 L. Tian, L. Zhang, Y. Liu, Y. He, Y. Zhu, R. Sun, S. Yi and J. Xiang, Clean production of ethyl levulinate from kitchen waste, *J. Cleaner Prod.*, 2020, **268**, 122296.

12 S. Kumar, M. R. Shamsuddin, M. S. A. Farabi, M. I. Saiman, Z. Zainal and Y. H. Taufiq- Yap, Production of methyl esters from waste cooking oil and chicken fat oil *via* simultaneous esterification and transesterification using acid catalyst, *Energy Convers. Manage.*, 2020, **266**, 113366.

13 K. Dhanalaxmi, R. Singuru, S. Mondal, L. Bai, B. M. Reddy, A. Bhaumik and J. Mondal, Magnetic Nanohybrid Decorated Porous Organic Polymer: Synergistic Catalyst for High Performance Levulinic Acid Hydrogenation, *ACS Sustainable Chem. Eng.*, 2017, **5**, 1033–1045.

14 J. Iglesias, J. A. Melero, G. Morales, M. Paniagua, B. Hernández, A. Osatiashtiani, A. F. Lee and K. Wilson, ZrO_2-SBA-15 catalysts for the one-pot cascade synthesis of GVL from furfural, *Catal. Sci. Technol.*, 2018, **8**, 4485–4493.

15 B. Banerjee, R. Singuru, S. K. Kundu, K. Dhanalaxmi, L. Bai, Y. Zhao, B. M. Reddy, A. Bhaumik and J. Mondal, Towards rational design of core–shell catalytic nanoreactor with high performance catalytic hydrogenation of levulinic acid, *Catal. Sci. Technol.*, 2016, **6**, 5102–5115.

16 R. Rodiansono, M. D. Astuti, K. Mustikasari, S. Husain and S. Sutomo, Recent progress in the direct synthesis of γ-valerolactone from biomass-derived sugars catalyzed by RANEY® Ni–Sn alloy supported on aluminium hydroxide, *Catal. Sci. Technol.*, 2020, **10**, 7768–7778.

17 X. Gao, X. Yu, L. Peng, L. He and J. Zhang, Magnetic Fe_3O_4 nanoparticles and ZrO_2-doped mesoporous MCM-41 as a monolithic multifunctional catalyst for γ- valerolactone production directly from furfural, *Fuel*, 2021, **300**, 120996.

18 W. Li, M. Li, H. Liu, W. Jia, X. Yu, S. Wang, X. Zeng, Y. Sun, J. Wei, X. Tang and L. Lin, Domino transformation of furfural to γ-valerolactone over SAPO-34 zeolite supported zirconium phosphate catalysts with tunable Lewis and Brønsted acid sites, *Mol. Catal.*, 2021, **506**, 111538.

19 Q. Peng, H. Wang, Y. Xia and X. Liu, One-pot conversion of furfural to gamma- valerolactone in the presence of

multifunctional zirconium alizarin red S hybrid, *Appl. Catal., A*, 2021, **621**, 118203.
20 T. Zhang, Y. Lu, W. Li, M. Su, T. Yang, A. Ogunbiyi and Y. Jin, One-pot production of γ- valerolactone from furfural using Zr-graphitic carbon nitride/H-b composite, *Int. J. Hydrogen Energy*, 2019, **44**, 14527–14535.
21 M. Li, J. Wei, G. Yan, H. Liu, X. Tang, Y. Sun, X. Zeng, T. Lei and L. Lin, Cascade conversion of furfural to fuel bioadditive ethyl levulinate over bifunctional zirconium- based catalysts, *Renewable Energy*, 2020, **147**, 916–923.
22 B. Chen, F. Li, Z. Huang, T. Lu, Y. Yuan and G. Yuan, Integrated Catalytic Process to Directly Convert Furfural to Levulinate Ester with High Selectivity, *ChemSusChem*, 2014, **7**, 202–209.
23 J. Wang, Y. Xu, B. Ding, Z. Chang, X. Zhang, Y. Yamauchi and K. C.-W. Wu, Confined Self-Assembly in Two-Dimensional Interlayer Space: Monolayered Mesoporous Carbon Nanosheets with In-Plane Orderly Arranged Mesopores and a Highly Graphitized Framework, *Angew. Chem., Int. Ed.*, 2018, **57**, 2894–2898.
24 E. Doustkhah, J. Lin, S. Rostamnia, C. Len, R. Luque, X. Luo, Y. Bando, K. C.-W. Wu, J. Kim, Y. Yamauchi and Y. Ide, Development of Sulfonic-Acid-Functionalized Mesoporous Materials: Synthesis and Catalytic Applications, *Chem.–Eur. J.*, 2019, **25**, 1614–1635.
25 R. K. Kankala, Y. H. Han, J. Na, C. H. Lee, Z. Sun, S. B. Wang, T. Kimura, Y. S. Ok, Y. Yamauchi, A. Z. Chen and K. C.-W. Wu, Nanoarchitectured Structure and Surface Biofunctionality of Mesoporous Silica Nanoparticles, *Adv. Mater.*, 2020, **32**, 1907035.
26 S. Karnjanakom, A. Bayu, P. Xiaoketi, X. Hao, S. Kongparakul, C. Samart, A. Abudula and G. Guan, Selective production of aromatic hydrocarbons from catalytic pyrolysis of biomass over Cu or Fe loaded mesoporous rod-like alumina, *RSC Adv.*, 2016, **6**, 50618–50629.
27 S. Karnjanakom, P. Phanthong, A. Bayu, P. Maneechakr, C. Samart, S. Kongparakul and G. Guan, Facile *In Situ* 5-EMF Synthesis and Extraction Processes from Catalytic Conversion of Sugar under Sustainable Long-Life Cycle, *ACS Sustainable Chem. Eng.*, 2020, **8**, 14867–14876.
28 L. Karam, M. Armandi, S. Casale, V. E. Khoury, B. Bonelli, P. Massiani and N. E. Hassan, Comprehensive study on the effect of magnesium loading over nickel-ordered mesoporous alumina for dry reforming of methane, *Energy Convers. Manage.*, 2020, **225**, 113470.
29 S. Karnjanakom, A. Bayu, X. Hao, S. Kongparakul, C. Samart, A. Abudula and G. Guan, Selectively catalytic upgrading of bio-oil to aromatic hydrocarbons over Zn, Ce or Ni- doped mesoporous rod-like alumina catalysts, *J. Mol. Catal. A: Chem.*, 2016, **421**, 235–244.
30 S. Karnjanakom, S. Kongparakul, C. Chaiya, P. Reubroycharoen, G. Guan and C. Samart, Biodiesel production from Hevea brasiliensis oil using SO_3H-MCM-41 catalyst, *J. Environ. Chem. Eng.*, 2016, **4**, 47–55.
31 S. T. Bararpour, D. Karami and N. Mahinpey, Utilization of mesoporous alumina-based supports synthesized by a surfactant-assisted technique for post-combustion CO_2 capture, *J. Environ. Chem. Eng.*, 2021, **9**, 105661.
32 Z. Tang, J. Liang, X. Li, J. Li, H. Guo, Y. Liu and C. Liu, Synthesis of flower-like Boehmite(γ-AlOOH) *via* a one-step ionic liquid-assisted hydrothermal route, *J. Solid State Chem.*, 2013, **202**, 305–314.
33 X. Xu, Q. Yu, Z. Lv, J. Song and M. He, Synthesis of high-surface-area rod-like alumina materials with enhanced Cr(VI) removal efficiency, *Microporous Mesoporous Mater.*, 2018, **262**, 140–147.
34 N. Ahmed and Z. N. Siddiqui, Mesoporous alumina sulphuric acid: A novel and efficient catalyst for on-water synthesis of functionalized 1,4-dihydropyridine derivatives *via* β- enaminones, *J. Mol. Catal. A: Chem.*, 2014, **394**, 232–243.
35 D. Li, L. Ruan, J. Sun, C. Wu, Z. Yan, J. Lin and Q. Yan, Facile growth of aluminum oxide thin film by chemical liquid deposition and its application in devices, *Nanotechnol. Rev.*, 2020, **9**, 876–885.
36 Z. Liu, Y. Qi, M. Gui, C. Feng, X. Wang and Y. Lei, Sulfonated carbon derived from the residue obtained after recovery of essential oil from the leaves of Cinnamomum longepaniculatum using Brønsted acid ionic liquid, and its use in the preparation of ellagic acid and gallic acid, *RSC Adv.*, 2019, **9**, 5142–5150.
37 S. Karnjanakom, A. Yoshida, A. Bayu, I. Kurnia, X. Hao, P. Maneechakr, A. Abudula and G. Guan, Bifunctional Mg-Cu-Loaded b-Zeolite: High Selectivity for the Conversion of Furfural into Monoaromatic Compounds, *ChemCatChem*, 2018, **10**, 3564–3575.
38 M. Rutkowska, I. Pacia, S. Basa, A. Kowalczyk, Z. Piwowarska, M. Duda, K. A. Tarach, K. Góra-Marek, M. Michalik, U. Díaz and L. Chmielarz, Catalytic performance of commercial Cu-ZSM-5 zeolite modified by desilication in NH_3-SCR and NH_3-SCO processes, *Microporous Mesoporous Mater.*, 2017, **246**, 193–206.
39 M. S. Tiwari, A. B. Gawade and G. D. Yadav, Magnetically separable sulfated zirconia as highly active acidic catalyst for selective synthesis of ethyl levulinate from furfuryl alcohol, *Green Chem.*, 2017, **19**, 963–976.
40 D. R. Chaffey, T. Bere, T. E. Davies, D. C. Apperley, S. H. Taylor and A. E. Graham, Conversion of levulinic acid to levulinate ester biofuels by heterogeneous catalysts in the presence of acetals and ketals, *Appl. Catal., B*, 2021, **293**, 120219.
41 L. Bui, H. Luo, W. R. Gunther and Y. Román-Leshkov, Domino Reaction Catalyzed by Zeolites with Brønsted and Lewis Acid Sites for the Production of g-Valerolactone from Furfural, *Angew. Chem., Int. Ed.*, 2013, **52**, 1–5.
42 M. Moreno-Recio, J. Santamaría-González and P. Maireles-Torres, Brönsted and Lewis acid ZSM-5 zeolites for the catalytic dehydration of glucose into 5-hydroxymethylfurfural, *Chem. Eng. J.*, 2016, **303**, 22–30.
43 S. K. Tyrlik, D. Szerszen, B. Kurzak and K. Bal, Concentrated water solutions of salts as solvents for reaction of carbohydrates. 1. Reactions of glucose promoted by

concentrated solutions of alkaline and alkaline-earth metal salts, *Starke*, 1995, **47**, 171–174.

44 C. García-Sanchoa, I. Fúnez-Núnezb, R. Moreno-Tostb, J. Santamaría-Gonzálezb, E. Pérez-Inestrosac, J. L. G. Fierroa and P. Maireles-Torres, Beneficial effects of calcium chloride on glucose dehydration to5-hydroxymethylfurfural in the presence of alumina as catalyst, *Appl. Catal., B*, 2017, **206**, 617–625.

45 S. Karnjanakom and P. Maneechakr, Designs of linear-quadratic regression models for facile conversion of carbohydrate into high value (5-(ethoxymethyl)furan-2-carboxaldehyde) fuel chemical, *Energy Convers. Manage.*, 2019, **196**, 410–417.

46 Y. Wang, Y. Huang, L. Liu, L. He, T. Li, C. Len and W. Yang, Molecular oxygen promoted synthesis of methyl levulinate from 5-hydroxymethylfurfural, *ACS Sustainable Chem. Eng.*, 2020, **8**, 14576–14583.

47 J. Jae, E. Mahmoud, R. F. Lobo and D. G. Vlachos, Cascade of Liquid-Phase Catalytic Transfer Hydrogenation and Etherification of 5-Hydroxymethylfurfural to Potential Biodiesel Components over Lewis Acid Zeolites, *ChemCatChem*, 2014, **6**, 508–513.

48 H. G. Bernala, P. Benitob, E. Rodríguez-Castellónc, A. M. R. Gallettia and T. Funaioli, Synthesis of isopropyl levulinate from furfural: Insights on a cascade production perspective, *Appl. Catal., A*, 2019, **575**, 111–119.

49 S. Karnjanakom, G. Guan, B. Asep, X. Hao, S. Kongparakul, C. Samart and A. Abudula, Catalytic Upgrading of Bio-Oil over Cu/MCM-41 and Cu/KIT-6 Prepared by β-Cyclodextrin-Assisted Coimpregnation Method, *J. Phys. Chem. C*, 2016, **120**, 3396–3407.

50 J. C. Waal, P. J. Kunkeler, K. Tan and H. Bekkum, Zeolite titanium beta: A selective catalyst in the meerwein-ponndorf-verley-oppenauer reactions, *Stud. Surf. Sci. Catal.*, 1997, **110**, 1015–1024.

51 C. Sievers, Y. Noda, L. Qi, E. M. Albuquerque, R. M. Rioux and S. L. Scott, Phenomena Affecting Catalytic Reactions at Solid–Liquid Interfaces, *ACS Catal.*, 2016, **6**, 8286–8307.

